JACS
JOURNAL OF THE AMERICAN CHEMICAL SOCIETY
Article
pubs.acs.org/JACS
Terms of Use

Oxygen Insertion into Metal Carbon Bonds: Formation of Methylperoxo Pd(II) and Pt(II) Complexes via Photogenerated Dinuclear Intermediates

Allan R. Petersen, Russell A. Taylor, Inmaculada Vicente-Hernández, Philip R. Mallender, Harriet Olley, Andrew J. P. White, and George J. P. Britovsek*

Department of Chemistry, Imperial College London, Exhibition Road, London, SW7 2AZ, U.K.

Supporting Information

ABSTRACT: Platinum(II) and palladium(II) complexes $[M(CH_3)(\mathbf{L})]SbF_6$ with substituted terpyridine ligands **L** undergo light-driven oxygen insertion reactions into metal methyl bonds resulting in methylperoxo complexes $[M(OOCH_3)(\mathbf{L})]SbF_6$. The oxygen insertion reactions occur readily for complexes with methyl ligands that are activated due to steric interaction with substituents (NH_2, NHMe or CH_3) at the 6,6″-positions on the terpyridine ligand. All complexes exhibit attractive intermolecular $\pi\cdots\pi$ or M···M interactions in the solid state and in solution, which lead to excited triplet dinuclear M−M complexes upon irradiation. A mechanism is proposed whereby a dinuclear intermediate is generated upon irradiation that has a weakened M−C bond in the excited state, resulting in the observed oxygen insertion reactions.

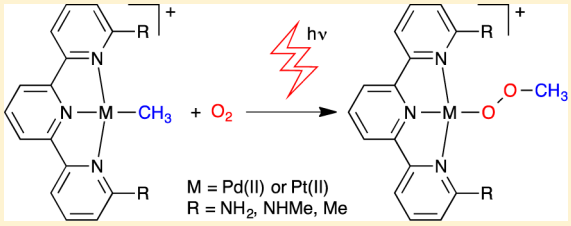

INTRODUCTION

The selective functionalization of methane and higher alkanes continues to be an important goal in catalysis research, especially with a view on the increasing availability of shale gas resources. The last three decades have witnessed tremendous advances in alkane C−H activation, in particular electrophilic activation reactions with late transition metals.[1−4] While C−H activation reactions of alkanes, including methane, are now well documented, the subsequent selective conversion of the metal carbon bond to useful products remains a challenge. Oxidation to alcohols or aldehydes, ideally with environmentally benign oxidants such as O_2 or H_2O_2, would be reactions of great interest, and considerable advances have been made in recent years.[5−9]

The oxidation of organometallic Pd(II) and Pt(II) complexes with a range of chemical oxidants has been reported,[10] for example, with Cl_2,[11] $PhICl_2$, $PhI(OAc)_2$,[12] $(PhIAr)(BF_4)$,[13] $PhI(CCSiMe_3)(OTf)$,[14] RSSR,[15] $(C_6H_4CMe_2O)ICF_3$,[16] and on several occasions dinuclear M(III)−M(III) intermediates were isolated and structurally characterized.[12,14,17,18] Dinuclear Pd(III)−Pd(III) complexes have also been implicated as intermediates in reactions where Pd(II) complexes have been used for catalytic C−Cl, C−Br and C−O bond formations.[12,19]

In contrast to the oxidants listed above, oxygen, in its triplet ground state, is relatively unreactive because reactions with substrates are spin-forbidden and require a triplet-singlet surface crossing on the reaction coordinate.[20] Examples of dioxygen *as a ligand* in d^8 metal complexes are plentiful and have been known for some time.[21] It has also been reported that certain Pt(II) complexes are able to act as oxygen sensitizers and generate singlet oxygen ($^1O_2$),[22−24] and in situ generated $^1O_2$ can react with organometallic complexes to generate peroxide complexes.[25,26] Examples of self-sensitization, whereby metal complexes generate $^1O_2$ and subsequently react with $^1O_2$ are also reported, either resulting in complexes with coordinated $^1O_2$,[27−29] or in further reactions, as observed in Pt(II) alkynyl and dithiolate complexes and more recently for a Pt(II) complex with an anthracenyl-bridged diphosphine ligand.[30−33]

We reported previously that a platinum(II) methyl complex $[Pt(CH_3)(\mathbf{1})](SbF_6)$ containing a tridentate 6,6″-diamino-substituted terpyridine ligand (**1**) reacts readily with O_2 upon exposure to light to give a methylperoxo platinum(II) complex $[Pt(OOCH_3)(\mathbf{1})](SbF_6)$ (eq 1).[34] Such oxygen insertion

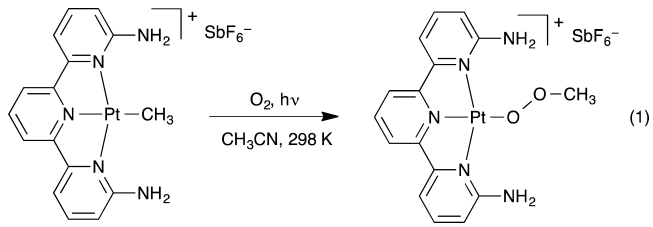

(1)

reactions into platinum(II) and palladium(II) methyl bonds are still very rare and the only other examples are those reported by Goldberg and co-workers.[35,36] The exact mechanism by which these oxygen insertion reactions operate is still not well understood and we present here our investigations into the role of the terpyridine ligand in these

Received: June 2, 2014
Published: September 8, 2014

dx.doi.org/10.1021/ja5055143 | J. Am. Chem. Soc. 2014, 136, 14089−14099

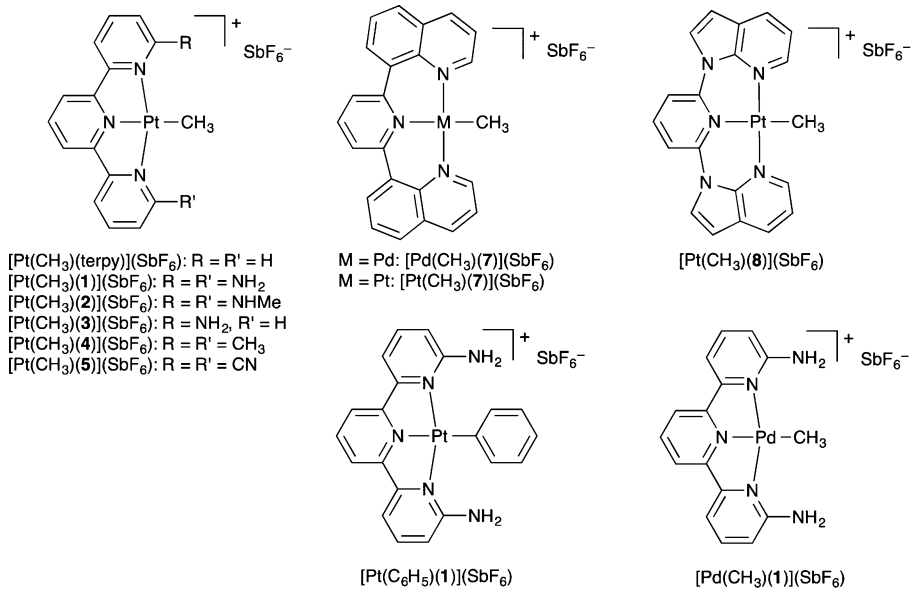

Figure 1. An overview of platinum(II) and palladium(II) complexes with substituted terpyridine and related ligands.

systems and the metal, as well as the need for light to observe fast oxygen insertion reactions. A mechanism for the insertion process is proposed, which incorporates the observations reported here, as well as the reaction of palladium and platinum complexes with other oxidants mentioned in the previous section. Excited dinuclear triplet state intermediates are invoked, which react with triplet oxygen generating superoxide and peroxide intermediates, eventually leading to the observed methylperoxo complexes.

RESULTS AND DISCUSSION

Synthesis of Ligands and Complexes. An overview of the ligands and complexes prepared in this study is given in Figure 1. The synthesis and characterization of all ligands and complexes are provided in the Supporting Information (SI) and the Experimental Section, respectively. The reaction of *trans*-$[PtCl(CH_3)(SMe_2)_2]$ with **1** and **3** in CH_2Cl_2 affords $[Pt(CH_3)(\mathbf{1})]Cl$ and $[Pt(CH_3)(\mathbf{3})]Cl$. Halide exchange reactions were carried out with $[Pt(CH_3)(\mathbf{1})]Cl$ using $AgSbF_6$ or $NaBAr^F{}_4$ ($BAr^F{}_4$ = *tetrakis*[3,5-*bis*(tri¯uoromethyl)-phenyl]borate) to give $[Pt(CH_3)(\mathbf{1})](SbF_6)$ and $[Pt(CH_3)(\mathbf{1})](BAr^F{}_4)$. The reaction of **2** with *trans*-$[PtCl(CH_3)(SMe_2)_2]$ did not go to completion. Similarly, **4** and **5** were unable to displace Me_2S from *trans*-$[PtCl(CH_3)(SMe_2)_2]$. The complexes $[Pt(CH_3)(\mathbf{2})](SbF_6)$ and $[Pt(CH_3)(\mathbf{4})](SbF_6)$ were therefore synthesized by the reaction of *trans*-$[PtCl(CH_3)(SMe_2)_2]$ with $AgSbF_6$ in acetone prior to addition of the ligand. The complexes $[Pt(CH_3)(\mathbf{5})](SbF_6)$, $[Pt(CH_3)(\mathbf{7})](SbF_6)$ and $[Pt(CH_3)(\mathbf{8})](SbF_6)$ were obtained by reacting *trans*-$[PtCl(CH_3)(SMe_2)_2]$ with $AgSbF_6$ and the ligand in acetone. Despite multiple attempts, complex $[Pt(CH_3)(\mathbf{6})](SbF_6)$ with the 6,6″-dimethoxyterpyridine ligand **6** could not be isolated cleanly and was always contaminated with unreacted ligand.

The platinum methyl ^1H NMR signals for the complexes $[Pt(CH_3)(\mathbf{L})](SbF_6)$ are typically observed between 0.5 and 2 ppm (see Experimental Section and Figures S1−S6 (SI)), but the chemical shift values can be strongly affected by concentration, temperature and solvents due to aggregation of the complexes in solution (vide infra). VT-^1H NMR analysis of $[Pt(CH_3)(\mathbf{1})]SbF_6$ in CD_3CN has shown a negative inversely proportional relationship between the chemical shift and temperature ($\delta \propto -1/T$).[37] The $^2J_{H-Pt}$ coupling constants are in the range of 68−78 Hz, but these satellites are often broadened due to chemical shift anisotropy. The ^{13}C NMR chemical shifts for the metal-bound methyl signals in complexes $[Pt(CH_3)(\mathbf{1})](SbF_6)$, $[Pt(CH_3)(\mathbf{2})](SbF_6)$ and $[Pt(CH_3)(\mathbf{4})](SbF_6)$ appear at −22.6, −21.6, and −12.6 ppm respectively, significantly upfield from those of $[Pt(CH_3)(terpy)](SbF_6)$, $[Pt(CH_3)(\mathbf{5})](SbF_6)$, $[Pt(CH_3)(\mathbf{7})](SbF_6)$ and $[Pt(CH_3)(\mathbf{8})](SbF_6)$, which are observed at −5.4, −3.1, −4.1, and −6.7 ppm, respectively (all in acetone-d_6). Similarly for palladium, the ^{13}C methyl signal is observed at −11.7 ppm for $[Pd(CH_3)(\mathbf{1})](SbF_6)$, compared to +5.8 and +5.7 ppm for $[Pd(CH_3)(terpy)](SbF_6)$ and $[Pd(CH_3)(\mathbf{7})](SbF_6)$, respectively. The upfield shift is believed to be a consequence of the steric repulsion between the methyl groups and the substituents in the 6,6″-positions, forcing the methyl groups out of the coordination plane.

Solid State Structures. The solid state structure of $[Pt(CH_3)(\mathbf{2})](SbF_6)$, which is similar to that of $[Pt(CH_3)(\mathbf{1})](SbF_6)$,[37] shows the platinum center to have a distorted square planar coordination geometry, the methyl carbon atom lying ca. 0.48 Å out of the N_3Pt plane due to steric repulsion between the methylamino substituents and the Pt−CH_3 group (Figure 2). The effect of this distortion is seen in both the N(1)−Pt−C angle, which at 168.90(10)° is significantly bent compared to the analogous angle of 179.0(3)° in $[Pt(CH_3)(terpy)](BPh_4)$ and in the Pt−C distance of 2.086(3) Å which is slightly longer than that seen in $[Pt(CH_3)(terpy)](BPh_4)$ [2.039(6) Å].[38] NOESY experiments have established that in solution, the *N*-methyl substituents in $[Pt(CH_3)(\mathbf{2})](SbF_6)$ are oriented such that C(13) and C(20) are pointing away from the Pt-methyl ligand, thereby minimizing steric repulsion, which is also the orientation seen here in the solid state.

The cations in $[Pt(CH_3)(\mathbf{2})](SbF_6)$ pack in a head-to-tail fashion due to attractive $\pi\cdots\pi$ interactions across two independent centers of symmetry to form an extended stack along the crystallographic *a* axis direction (Figure 3). The centroid···centroid, mean interplanar separations and ring inclinations are ca. 3.71, 3.53 Å and 5° for the N(15)···N(1)

dx.doi.org/10.1021/ja5055143 | J. Am. Chem. Soc. 2014, 136, 14089−14099

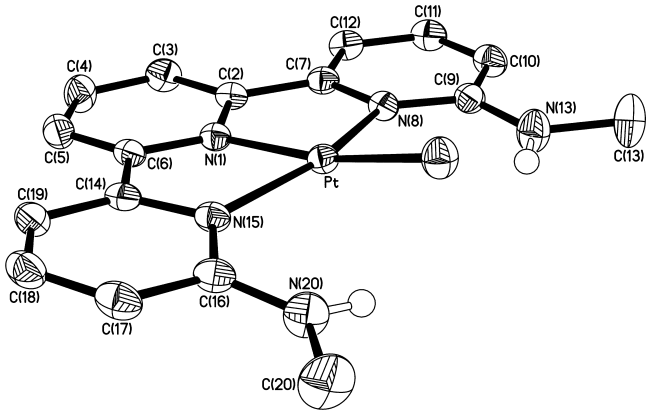

Figure 2. Molecular structure of $[Pt(CH_3)(\mathbf{2})](SbF_6)$ (50% probability ellipsoids). Hydrogen atoms and the anion have been omitted for clarity.

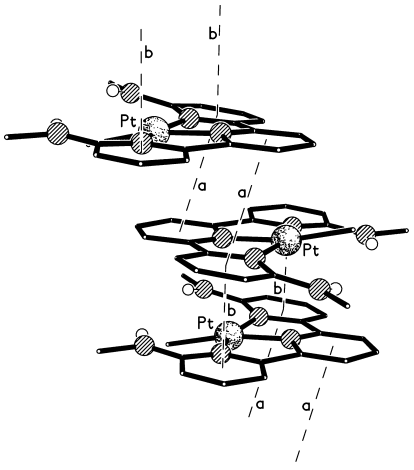

Figure 3. Part of one of the $\pi-\pi$ linked stacks of cations along the *a* axis direction present in the crystal of $[Pt(CH_3)(\mathbf{2})](SbF_6)$. The $\pi-\pi$ stacking interactions have centroid···centroid and mean interplanar separations (Å) of (a) 3.71, 3.53, and (b) 3.68, 3.41, respectively.

contact, and ca. 3.68, 3.41 Å and 5° respectively for the N(15)···N(8) contact (interactions a and b, respectively).

The structure of $[Pt(CH_3)(\mathbf{7})](SbF_6)$ was found to contain four crystallographically independent cations (**A**–**D**) in the asymmetric unit, all of which have very similar conformations, though **A** and **C** are enantiomers of **B** and **D** (cation $[Pt(CH_3)(\mathbf{7})]^+$-**A** is shown in Figure 4, while the remaining three are shown in Figures S18–S20 (SI)). Selected bond lengths and angles for the four cations are comparable to those previously calculated by DFT for $[Pt(Cl)(\mathbf{7})]^+$.[39]

The structure of $[Pt(CH_3)(\mathbf{8})](SbF_6)$ contains just one independent cation (Figure 5). Both $[Pt(CH_3)(\mathbf{7})](SbF_6)$ and $[Pt(CH_3)(\mathbf{8})](SbF_6)$ show a square planar geometry, but the methyl carbon atom lies much closer to the coordination plane, being only ca. 0.03–0.13 and 0.21 Å respectively out of the N_3Pt plane, compared to ca. 0.53 and 0.48 Å for $[Pt(CH_3)(\mathbf{1})](SbF_6)$ and $[Pt(CH_3)(\mathbf{2})](SbF_6)$. The corresponding N(1)–Pt–CH_3 angles are 176.9(4)–179.3(4)° for $[Pt(CH_3)(\mathbf{7})](SbF_6)$ (**A**–**D**), and 175.74(18)° for $[Pt(CH_3)(\mathbf{8})](SbF_6)$, cf. 167.31(14) and 168.90(10)° for $[Pt(CH_3)(\mathbf{1})](SbF_6)$ and $[Pt(CH_3)(\mathbf{2})](SbF_6)$ respectively. Compared to $[Pt(CH_3)(\mathbf{1})](SbF_6)$ and $[Pt(CH_3)(\mathbf{2})](SbF_6)$, the ligands in $[Pt(CH_3)(\mathbf{7})](SbF_6)$ and $[Pt(CH_3)(\mathbf{8})](SbF_6)$ are significantly twisted

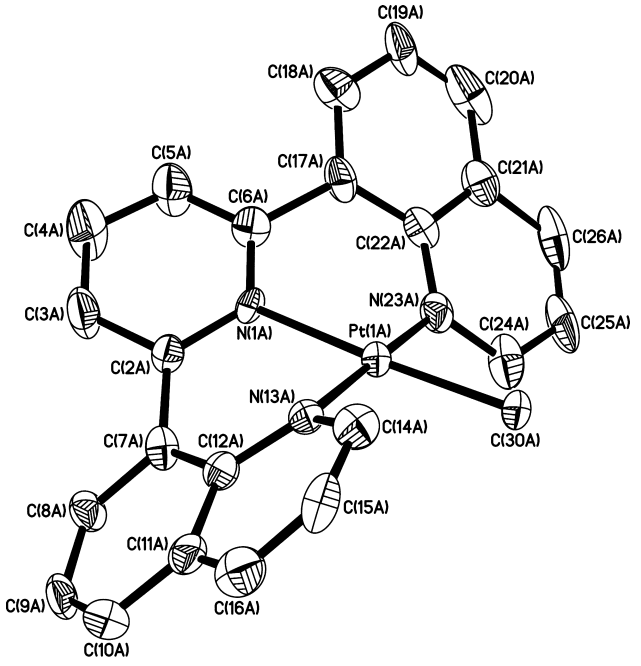

Figure 4. Molecular structure of complex $[Pt(CH_3)(\mathbf{7})](SbF_6)$ (**A**) (50% probability ellipsoids). Hydrogen atoms and the anion have been omitted for clarity.

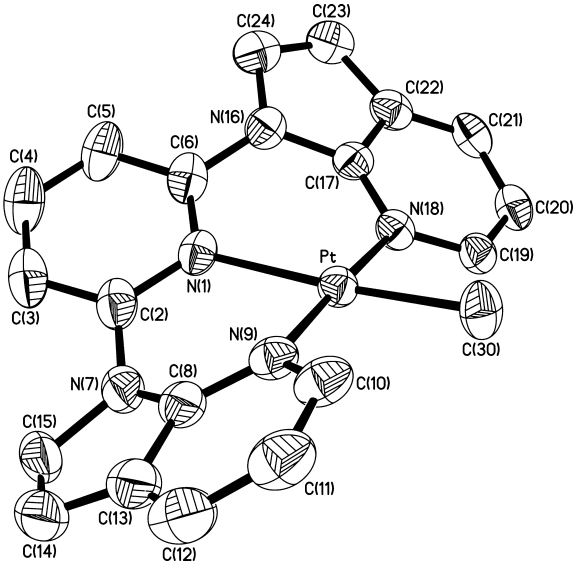

Figure 5. Molecular structure of complex $[Pt(CH_3)(\mathbf{8})](SbF_6)$ (50% probability ellipsoids). Hydrogen atoms and the anion have been omitted for clarity.

(see Supporting Information for more details). This was also seen in the related complexes $[Ru(\mathbf{7})_2](PF_6)_2$, $[Ru(\mathbf{7})(MeCN)_3](PF_6)_2$ and $[Cu(\mathbf{8})(NO_3)_2]$,[40–42] although a different coordination mode was recently observed in $[Zn(\mathbf{8})(OTf)_2]$.[43] The larger bite angle of the 6-membered *N,N′* chelate rings in $[Pt(CH_3)(\mathbf{7})](SbF_6)$ and $[Pt(CH_3)(\mathbf{8})](SbF_6)$ allows the *trans* N–Pt–N angles to approach 180°, being 177.7(4)-178.4(5), and 177.29(13)° in $[PtCH_3(\mathbf{7})](SbF_6)$ (**A**–**D**) and $[PtCH_3(\mathbf{8})](SbF_6)$, respectively, cf. 159.25(12) and 158.73(9)° for $[Pt(CH_3)(\mathbf{1})](SbF_6)$ and $[Pt(CH_3)(\mathbf{2})](SbF_6)$, respectively.

dx.doi.org/10.1021/ja5055143 | J. Am. Chem. Soc. 2014, 136, 14089–14099

Square planar palladium(II) and platinum(II) complexes, as well as other d^8 metal complexes are well-known to form weakly associated dimers or extended aggregates in the solid state and in solution, due to a combination of attractive M···M and $\pi\cdots\pi$ interactions.[44−49] These interactions have also been observed in terpyridine palladium(II) and platinum(II) complexes.[37,38,50−55] For example, predominantly $\pi\cdots\pi$ interactions are seen in the solid state structures of complexes $[Pt(CH_3)(\mathbf{2})](SbF_6)$, $[Pt(CH_3)(\mathbf{7})](SbF_6)$ and $[Pt(CH_3)(\mathbf{8})](SbF_6)$ (see Figure 3 and Figures S15−S17 (SI)), whereas a Pt···Pt interaction was observed in $[Pt(OOCH_3)(\mathbf{1})](SbF_6)$ (Pt···Pt separation 3.20 Å).[34] Such interactions are believed to be important in the light-driven alkyl exchange reactions observed with complexes $[Pt(CH_3)(\mathbf{1})](SbF_6)$ and $[Pd(CH_3)(\mathbf{1})](SbF_6)$, and may also be of importance for the reactivity with oxygen seen here.[37]

Reactivity with Oxygen. $[Pt(CH_3)(\mathbf{1})](SbF_6)$ reacts with oxygen under the influence of light to give the methylperoxo complex $[Pt(OOCH_3)(\mathbf{1})](SbF_6)$ (see eq 1). The insertion reaction occurs within minutes at room temperature using sunlight or a UV light source (365 nm, 100W), whereas in the absence of light the half-life is approximately 13 h.[34] $[Pt(CH_3)(\mathbf{1})](SbF_6)$ is soluble in acetone and acetonitrile and the dioxygen insertion reactions have been carried out in these polar solvents. In order to investigate the insertion reaction in other solvents, complexes $[Pt(CH_3)(\mathbf{1})]Cl$ and $[Pt(CH_3)(\mathbf{1})](BAr^F{}_4)$ with different counteranions have been employed. $[Pt(CH_3)(\mathbf{1})]Cl$ was dissolved in D_2O at room temperature and the addition of O_2 and light resulted in a facile O_2 insertion to give $[Pt(OOCH_3)(\mathbf{1})]Cl$. The Pt−$CH_3$ signal at 1.00 ppm disappears over the course of 20 min and a new signal emerges at 3.32 ppm, together with a new set of terpyridine signals. Similarly, when a solution of $[Pt(CH_3)(\mathbf{1})](BAr^F{}_4)$ in $CDCl_3$ was exposed to dioxygen and light, the Pt−CH_3 signal at 1.62 ppm disappears and a new singlet for $[Pt(OOCH_3)(\mathbf{1})](BAr^F{}_4)$ is formed at 3.81 ppm (see Figure S8 (SI)). These observations in D_2O and $CDCl_3$ are analogous to the O_2 insertion reactions of $[Pt(CH_3)(\mathbf{1})](SbF_6)$ in $(CD_3)_2CO$ and CD_3CN, but they do make some important points. First, if Pt−CH_3 heterolysis was involved in the insertion mechanism, methyl cations or anions would most likely be intercepted in an aqueous environment resulting in methane or methanol as potential byproducts, but neither of these is observed. Second, if Pt−CH_3 homolysis was involved in the photochemical reaction, the formation of radicals could lead to other complexes in chlorinated solvents such as $CDCl_3$, for example $[Pt(Cl)(\mathbf{1})]^+$, as seen in other reactions.[15,56,57] The formation of $[PtCl(\mathbf{1})](SbF_6)$, which was independently prepared and reported previously,[34] was never observed. These observations therefore favor an intramolecular insertion mechanism.

The possibility of oxygen insertion into Pt-aryl bonds was investigated by adding oxygen to a solution of $[Pt(C_6H_5)(\mathbf{1})](SbF_6)$ in CD_3CN and exposure to sunlight. The same conditions as for $[Pt(CH_3)(\mathbf{1})](SbF_6)$ were used, but no O_2 insertion reaction was observed. More forcing conditions such as exposure to UV-light for 1 h in $(CD_3)_2CO$ or CD_3CN and heating the solution at 50 °C for 30 min, did not result in O_2 insertion. A solution of $[Pt(C_6H_5)(\mathbf{1})](SbF_6)$ in $(CD_3)_2CO$ with 5 bar of oxygen pressure and exposure to light did not lead to any reaction, even after 24 h. It was concluded that O_2 does not insert into the Pt−C bond of $[Pt(C_6H_5)(\mathbf{1})](SbF_6)$. The Pt−C bond dissociation energy for platinum(II) phenyl complexes is approximately 50 kcal/mol, whereas for platinum(II) methyl complexes approximately 36 kcal/mol.[58−61] Furthermore, the steric hindrance caused by the NH_2 substituents in complex $[Pt(CH_3)(\mathbf{1})](SbF_6)$ weakens the Pt−C bond even further, as can be seen from the N_{pyr}−Pt−C angles, which are 178.55(14)° and 167.31(14)° for complexes $[Pt(C_6H_5)(\mathbf{1})](SbF_6)$ and $[Pt(CH_3)(\mathbf{1})](SbF_6)$, respectively. Noteworthy, oxygen insertion has been observed for a chromium(II)-phenyl complex leading to the formation of a $[Cr^{IV}(O)(OPh)]$ complex.[62]

$[Pt(CH_3)(\mathbf{2})](SbF_6)$ with methylamino substituents inserts O_2 readily into the Pt−CH_3 bond to generate $[Pt(OOCH_3)(\mathbf{2})](SbF_6)$ (see Figure S9 (SI)). In order to investigate the steric effects in more detail, the platinum(II) complex $[Pt(CH_3)(\mathbf{3})](SbF_6)$ with only one NH_2 substituent was prepared. Oxygen was introduced to a solution of $[Pt(CH_3)(\mathbf{3})](SbF_6)$ in CD_3CN, but no insertion reaction occurred upon exposure to sunlight (up to 19 h). It can be concluded that both amino groups are required for oxygen insertion to take place in these terpyridine platinum(II) methyl complexes.

To establish whether the NH_2 or NHMe substituents are required for steric or for electronic reasons, 6,6″-dimethyl terpyridine complex $[Pt(CH_3)(\mathbf{4})](SbF_6)$ was prepared. While methyl groups are sterically similar to amino groups, the UV−vis spectra of $[Pt(CH_3)(\mathbf{4})](SbF_6)$ and $[Pt(CH_3)(\mathbf{1})](SbF_6)$ indicate that the methyl groups have a significantly different electronic effect, more similar to the hydrogen substituents in terpy (vide supra). Related observations were reported for 4′-methyl-terpy when compared to terpy.[63] A solution of $[Pt(CH_3)(\mathbf{4})](SbF_6)$ in $(CD_3)_2CO$ was saturated with O_2 and exposed to light. The Pt−CH_3 signal at 1.76 ppm disappears and a new singlet for $[Pt(OOCH_3)(\mathbf{4})](SbF_6)$ appears at 3.80 ppm (see Figure S10 (SI)). Considering that $[Pt(CH_3)(terpy)](SbF_6)$ does not insert dioxygen, we propose that the reactions of $[Pt(CH_3)(\mathbf{4})](SbF_6)$ and also of $[Pt(CH_3)(\mathbf{1})](SbF_6)$ with oxygen are due to steric effects.

In line with the steric argument, $[Pt(CH_3)(\mathbf{5})](SbF_6)$ with sterically less encumbered cyanide substituents, does not react with oxygen after exposure to sunlight. Furthermore, the reaction of complexes $[Pt(CH_3)(\mathbf{7})](SbF_6)$ and $[Pt(CH_3)(\mathbf{8})](SbF_6)$ with oxygen, which were carried out at 1 bar pressure and at 5 bar O_2 pressure did not result in oxygen insertion after exposure to sunlight.

The addition of oxygen and sunlight to the palladium complex $[Pd(CH_3)(\mathbf{1})](SbF_6)$ in CD_3CN results in oxygen insertion, whereby the Pd−CH_3 signal at 0.82 ppm disappears within minutes and a new singlet at 3.72 ppm appears, assigned to the methylperoxo palladium complex $[Pd(OOCH_3)(\mathbf{1})](SbF_6)$ (Figure S11 (SI)). The NH_2 resonance, observed as a broad resonance at 5.8 ppm for $[Pd(CH_3)(\mathbf{1})](SbF_6)$, becomes very broad and is not detected at room temperature. Hydrogen bonding between the NH_2 protons and the methylperoxo ligand decreases the rate of exchange between the *endo*- and *exo*-NH_2 protons to the point of coalescence, as previously observed for the analogous platinum(II) complex $[Pt(OOCH_3)(\mathbf{1})](SbF_6)$. The methylperoxo palladium complex $[Pd(OOCH_3)(\mathbf{1})](SbF_6)$ is remarkably stable in CD_3CN and no decomposition was observed within 8 h (see Figure S7 (SI)).

It can be concluded at this stage that only the methyl platinum(II) and palladium(II) complexes containing terpyridine ligands with either two amino, two methylamino or two methyl substituents (ligands **1**, **2** and **4**) react with oxygen after

dx.doi.org/10.1021/ja5055143 | J. Am. Chem. Soc. 2014, 136, 14089−14099

exposure to light at room temperature (eq 2). These four complexes have in common that they all possess two sp^2 (NH_2 or NHMe) or sp^3 (CH_3) hybridized substituents in the 6,6″-positions. We postulate that the steric interference with the metal-bound methyl results in a weakening of the metal carbon bond and activation toward oxygen insertion. All other complexes investigated here do not have these steric requirements and consequently do not insert O_2. The steric interaction most likely results in a weakening of the M−C bond, either raising the ground state energy for these complexes, or lowering the transition state energy for the O_2 insertion reaction. The methylperoxo complexes are generally unstable and decompose within several hours or less. A common decomposition route appears to be the elimination of formaldehyde and the generation of a metal(II) hydroxo complex. Further studies on this decomposition reaction are underway.

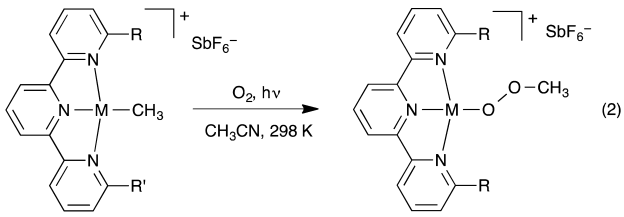

[PtCH3(1)](SbF6): R = R' = NH2
[PtCH3(2)](SbF6): R = R' = NHMe
[PtCH3(4)](SbF6): R = R' = CH3
[PdCH3(1)](SbF6): R = R' = NH2

[PtOOCH3(1)](SbF6): R = R' = NH2
[PtOOCH3(2)](SbF6): R = R' = NHMe
[PtOOCH3(4)](SbF6): R = R' = CH3
[PdOOCH3(1)](SbF6): R = R' = NH2

Crossover Experiments. Initial observations suggested that the strong chromophore in the diamino-substituted terpy complexes may be responsible for the conversion of triplet oxygen into singlet oxygen under the influence of light. Terpy complexes without 6,6″-diamino substituents such as [Pt(CH_3)(terpy)](SbF_6) or [Pd(CH_3)(terpy)](SbF_6) show a markedly different UV−vis spectrum and no insertion of oxygen is observed with these complexes. If [Pt(CH_3)(**1**)](SbF_6) acts as a photosensitizer and $^1O_2$ is generated in situ, this singlet oxygen might also react with other complexes such as [Pt(CH_3)(terpy)](SbF_6) to form the methylperoxo complex [Pt($OOCH_3$)(terpy)](SbF_6). To investigate this possibility, a mixture of approximately equimolar amounts of [Pt(CH_3)(terpy)](SbF_6) and [Pt(CH_3)(**1**)](SbF_6) in CD_3CN was saturated with oxygen (Scheme 1). After exposure to light, the reaction was monitored by ^1H NMR spectroscopy (see Figure S12 (SI)). The methyl signal of [Pt(CH_3)(**1**)](SbF_6) at 1.51 ppm disappears and a new singlet for [Pt($OOCH_3$)(**1**)](SbF_6) appears at 3.65 ppm, whereas the methyl signal of [Pt(CH_3)(terpy)](SbF_6) at 1.04 ppm remains unchanged. Furthermore, the addition of oxygen and light to a solution of [Pt(CH_3)(**1**)](SbF_6) in CD_3CN in the presence of an excess of tetramethylpiperidine (TEMP), a known singlet oxygen scavenger,[64] resulted in a clean conversion to the methyl peroxo complex. We therefore conclude that *free* singlet oxygen, which has a lifetime of 600 ± 33 μs in CD_3CN,[65] if generated under these conditions, is not involved in the oxygen insertion reaction.

Labeling studies have shown that methyl exchange takes place between [Pt(CD_3)(**1**)](SbF_6) and [Pt(CH_3)(terpy)](SbF_6) in CD_3CN when exposed to UV light (in the absence of oxygen). The half-life for this exchange process is approximately 17 min under the conditions used (room temperature, 365 nm, 100W).[37] Addition of oxygen to an equilibrium mixture of the four complexes and further exposure to light results in the formation of [Pt($OOCH_3$)(**1**)](SbF_6) and [Pt($OOCD_3$)(**1**)](SbF_6), together with unreacted [Pt(CH_3)(terpy)](SbF_6) and [Pt(CD_3)(terpy)](SbF_6). Despite the fact that [Pt(CD_3)(**1**)](SbF_6) and [Pt(CH_3)(terpy)](SbF_6) can readily exchange methyl groups, only complexes with disubstitued terpy ligands insert dioxygen. These results do not support a radical-based mechanism where methyl or methylperoxo radicals are involved, neither for the methyl exchange nor for the oxygen insertion reaction. Furthermore, there is no exchange of methyl with methylperoxo ligands between [Pt($OOCH_3$)(**1**)](SbF_6) and [Pt(CH_3)(terpy)](SbF_6). The ability to insert dioxygen appears to be an inherent property of disubstituted terpy complexes and not for terpy complexes, even though the methyl groups can be exchanged quite readily.

An equimolar solution of [Pt(CD_3)(**1**)](SbF_6) and [Pd(CH_3)(**1**)](SbF_6) in acetone-d_6 was saturated with dioxygen and exposed to light. The initial ^1H NMR spectrum displays a Pd−CH_3 signal at 1.02 ppm. When the solution is exposed to light the Pd−CH_3 peak disappears and two new signals appear at 3.63 and 3.70 ppm, assigned to $PtOOCH_3$ and $PdOOCH_3$ complexes (see Figure 6). A complementary ^2H NMR experiment in nondeuterated acetone shows the methylperoxo signals of [Pt($OOCD_3$)(**1**)](SbF_6) and [Pd($OOCD_3$)(**1**)](SbF_6) (see Figure S13 (SI)). The two complexes [Pt(CD_3)(**1**)](SbF_6) and [Pd(CH_3)(**1**)](SbF_6) undergo methyl exchange with a half-life of approximately 11 min.[37] Both complexes can insert oxygen and consequently all four methylperoxo complexes are obtained.

UV−Vis Spectroscopy. The different charge transfer behavior of [Pt(CH_3)(**1**)](SbF_6) compared to [Pt(CH_3)(terpy)](SbF_6) was thought to be related to the different reactivity toward oxygen, as [Pt(CH_3)(**1**)](SbF_6) reacts readily with O_2 to give a methyl peroxo complex, whereas [Pt(CH_3)(terpy)](SbF_6) does not. In contrast, the UV−vis spectra of [Pt(CH_3)(**1**)](SbF_6) and the phenyl complex [Pt(C_6H_5)(**1**)](SbF_6) are rather similar,[37] but [Pt(CH_3)(**1**)](SbF_6) readily

Scheme 1. Oxygen Addition to a Mixture of [Pt(CH_3)(1)](SbF_6) and [Pt(CH_3)(terpy)](SbF_6) in CD_3CN

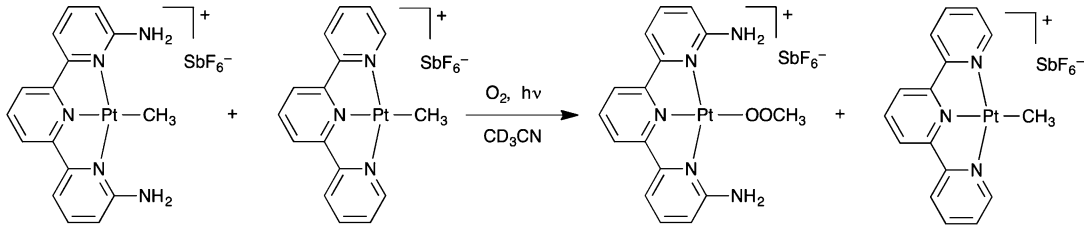

[Pt(CH3)(1)](SbF6) [Pt(CH3)(terpy)](SbF6) [Pt(OOCH3)(1)](SbF6) [Pt(CH3)(terpy)](SbF6)

dx.doi.org/10.1021/ja5055143 | J. Am. Chem. Soc. 2014, 136, 14089−14099

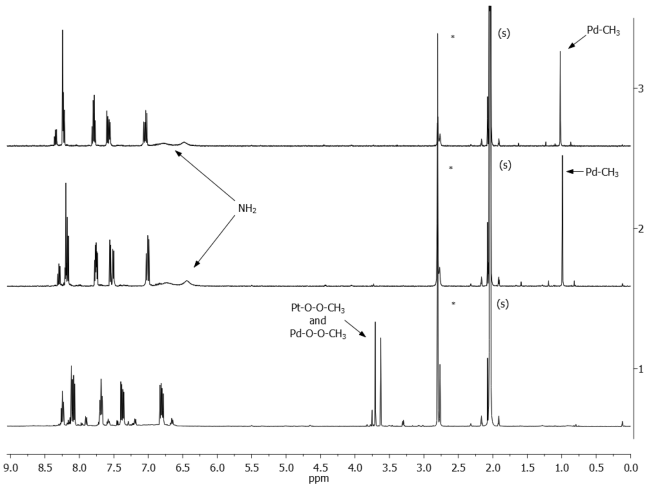

Figure 6. ^{1}H NMR spectrum at 400 MHz, 298 K of [Pt(CD$_3$)(**1**)](SbF$_6$) and [Pd(CH$_3$)(**1**)](SbF$_6$) in acetone-d_6 (s) (top). ^{1}H NMR spectrum of the same sample saturated with dioxygen (middle). ^{1}H NMR spectrum of the same sample saturated with dioxygen after exposure to light (bottom). * = H$_2$O and HDO.

inserts oxygen, whereas [Pt(C$_6$H$_5$)(**1**)](SbF$_6$) does not. The UV–vis spectra of all complexes prepared in this study have been collected in an attempt to identify a potential correlation between the oxygen insertion ability of the metal complexes and their electronic properties.

The UV–vis spectra of [Pt(CH$_3$)(**2**)](SbF$_6$), [Pt(CH$_3$)(**3**)](SbF$_6$) and [Pt(CH$_3$)(**4**)](SbF$_6$) are collected in Figure 7,

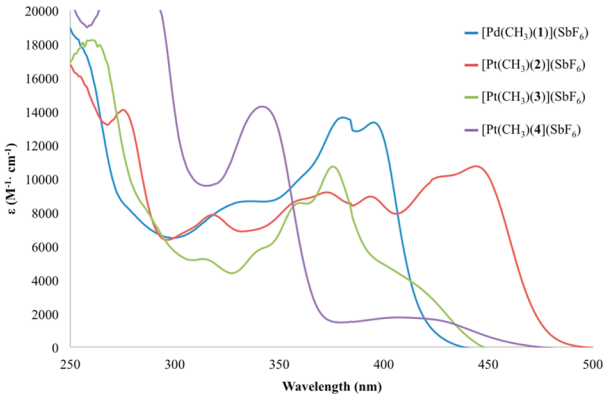

Figure 7. UV–vis spectra of [Pd(CH$_3$)(**1**)](SbF$_6$), [Pt(CH$_3$)(**2**)](SbF$_6$), [Pt(CH$_3$)(**3**)](SbF$_6$) and [Pt(CH$_3$)(**4**)](SbF$_6$) in CH$_3$CN at 298 K.

together with the spectrum of the palladium complex [Pd(CH$_3$)(**1**)](SbF$_6$). The methylamino groups in complex [Pt(CH$_3$)(**2**)](SbF$_6$) are more basic, which will increase the electron density at the metal center compared to [Pt(CH$_3$)(**1**)](SbF$_6$) and shift the MLCT band to higher wavelengths. Only one amino group in [Pt(CH$_3$)(**3**)](SbF$_6$) results in a shift of the MLCT absorption approximately halfway between [Pt(CH$_3$)(**1**)](SbF$_6$) and the terpy complex. The spectrum of the dimethylterpy complex [Pt(CH$_3$)(**4**)](SbF$_6$) resembles that of [Pt(CH$_3$)(terpy)](SbF$_6$), which indicates a negligible electronic effect caused by the methyl substituents.

The absorption maxima of [Pt(CH$_3$)(**7**)](SbF$_6$) and [Pd(CH$_3$)(**7**)](SbF$_6$) are comparable (λ_{max} = 344 and 340 nm, respectively) and are similar to the reported spectrum of [PtCl(**7**)]$^+$ with λ_{max} = 347 nm, which indicates that these absorptions are largely ligand-based (see Figure S14 (SI)).[39] The spectrum of [Pt(CH$_3$)(**8**)](SbF$_6$) exhibits a broad absorption with λ_{max} = 326 nm, higher in energy than [Pt(CH$_3$)(**7**)](SbF$_6$) and close to the value reported for [PtCl(**8**)]$^+$ (λ_{max} = 336 nm).[39] The higher energy band is explained by the LUMO being largely localized on the central pyridine ring and is not delocalized across the entire ligand, as found for [PtCl(**7**)]$^+$.[39]

Considering that [Pt(CH$_3$)(**1**)](SbF$_6$), [Pt(CH$_3$)(**2**)](SbF$_6$) and [Pt(CH$_3$)(**4**)](SbF$_6$) insert oxygen, whereas [Pt(CH$_3$)(**3**)](SbF$_6$) and [Pt(C$_6$H$_5$)(**1**)](SbF$_6$) do not, we can conclude that there is no apparent correlation between the electronic spectra of these complexes and their reactivity toward oxygen.

Mechanistic Considerations. We initially proposed a mechanism for the insertion of oxygen in the case of complex [Pt(CH$_3$)(**1**)](SbF$_6$) that proceeds via ^{3}O$_2$ sensitization and generation of ^{1}O$_2$, followed by insertion of ^{1}O$_2$ into the Pt methyl bond.[34] However, additional experimental evidence presented here has indicated that the exact mechanism is rather more complicated. The first oxygen insertion crossover experiment, discussed in the previous section, between [Pt(CH$_3$)(**1**)](SbF$_6$) and [Pt(CH$_3$)(terpy)](SbF$_6$) has shown that *free* ^{1}O$_2$, if generated by these complexes, is not responsible for the observed O$_2$ insertion reaction. This would suggest that, rather than triplet oxygen being converted into singlet oxygen, the singlet platinum(II) or palladium(II) complexes must be converted into a triplet state, in order to react with triplet oxygen.

Square planar palladium(II) and platinum(II) complexes, as well as other d^8 metal complexes, are well-known to form dimers or extended aggregates in the solid state and in solution due to a combination of attractive M···M and $\pi\cdots\pi$ interactions.[11,44−49] Such interactions have also been observed in terpyridine palladium(II) and platinum(II) complexes,[38,50−53,66−68] and $\pi\cdots\pi$ interactions have been seen for example in the solid state in structures of complexes [PtCH$_3$(**1**)](SbF$_6$) and [PtCH$_3$(**2**)](SbF$_6$), whereas a Pt···Pt interaction is observed in [Pt(OOCH$_3$)(**1**)](SbF$_6$) (Pt···Pt = 3.1999(5) Å).[34] Electronic excitation of these loosely associate dimeric [M···M] complexes results in electron transfer from the HOMO to the LUMO and the formation of an excited dinuclear triplet state complex ^{3}[M$_2$]*.[46,47,69] Electron transfer from the HOMO, a d$_{z^2}$ σ* M···M antibonding orbital, can either occur to a p$_z$ σ M···M bonding orbital, resulting in a M–M bond order of 1 (class (i) dimers), or to a ligand-based orbital, resulting in a bond order of 0.5 (class (ii) dimers).[48,70] The former is typical for Pt(II), Rh(I) and Ir(I) complexes, whereas the latter is more common for Pd(II) complexes, but has recently also been observed for Pt(II).[48] Formal removal of electrons from the HOMO by electrochemical methods has shown that a stepwise oxidation from [M(II)···M(II)] to [M(III)–M(III)] complexes can occur for palladium(II) and platinum(II)[48,49,70] or from [M(I)···M(I)] to [M(II)–M(II)] complexes in the case of rhodium and iridium.[71] Stable [M(III)–M(III)] complexes with a formal d^7 electron configuration can be formed by chemical oxidation of [M(II)···M(II)] complexes.[12,13,18,19,72]

Taking all this information together, we propose a mechanism shown in Scheme 2 for the insertion of oxygen into a metal methyl bond. Upon exposure to light, the loosely aggregated d^8 Pd(II) or Pt(II) methyl complexes [(M(II)···M(II)] generate an excited dinuclear triplet complex ^{3}[M$_2$]*

dx.doi.org/10.1021/ja5055143 | J. Am. Chem. Soc. 2014, 136, 14089−14099

Scheme 2. Proposed Mechanism for the Light-Driven O_2 Insertion into M−CH_3 Bonds (M = Pd or Pt)

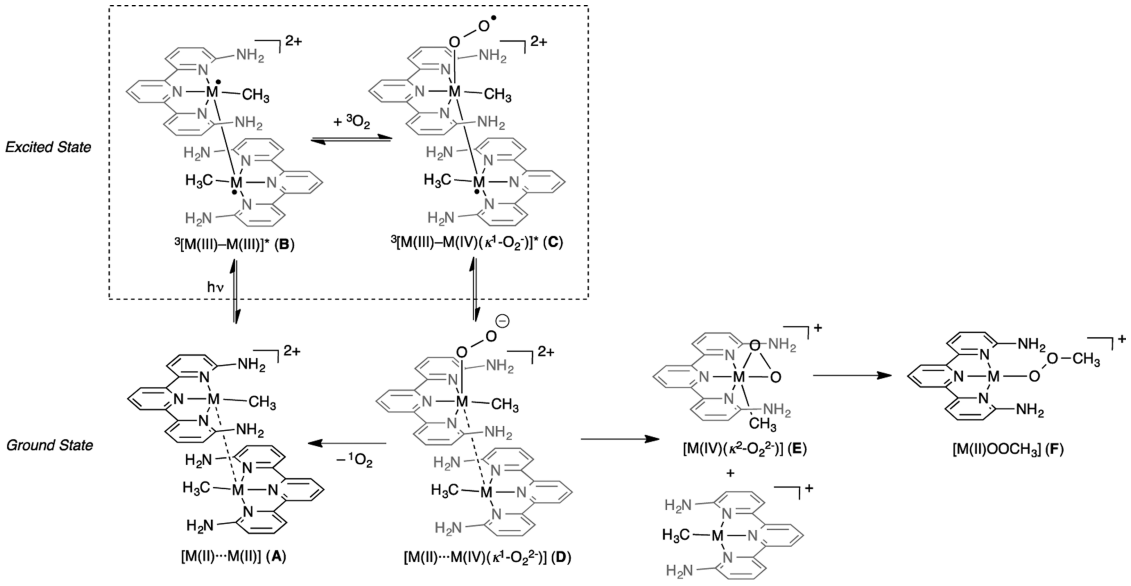

(M = Pd or Pt) with a metal−metal bond. The assignment of oxidation states for these excited state dinuclear complexes is nontrivial,[18,73] yet we do believe it is helpful to try and assign oxidation states for the metal centers in the intermediates, as electron bookkeeping helps to rationalize the stepwise reduction of oxygen to peroxide. While no formal oxidation (as in removal of electrons) takes place upon excitation, the electron transfer form the HOMO generates a triplet state complex which can be viewed as a ^{3}[M(III)−M(III)]* complex (**B**), with a formal d^7 M(III) configuration at each metal center and two unpaired electrons in different orbitals. This triplet state complex can react with triplet oxygen to give a dinuclear triplet intermediate complex $^3[M_2(O_2)]^*$, which can be described as a ^{3}[M(III)−M(IV)(κ^1-O_2^-)]* complex (**C**) following electron transfer from one of the metal centers to generate an end-on monoanionic superoxide ligand. Noteworthy, in a recent report on the reaction of a Pd(II) dimethyl complex with oxygen, a mononuclear palladium(III) superoxide complex [L_nPd(III)(κ^1-O_2^-)] was proposed as a reaction intermediate.[74]

The triplet dinuclear superoxide complex **C** subsequently reverts to a singlet ground state complex [M(II)···M(IV)(κ^1-O_2^{2-})] (**D**) with an end-on peroxide ligand.[75] In the ground state, the electron-rich M(II) complex acts as a ligand to stabilize the, otherwise five-coordinate, M(IV) complex with the end-on peroxide ligand.[14,15] This M(IV) complex **D** can eliminate singlet oxygen and revert back to the M(II) starting complex, which would be the conventional Type II mechanism by which photosensitizers convert triplet oxygen into singlet oxygen.[76] Alternatively, the end-on peroxide complex **D** converts to a monomeric complex [M(IV)(κ^2-O_2^{2-})] (**E**) with a side-on peroxide ligand, under elimination of the stabilizing M(II) starting complex. A similar oxidation of a dinuclear d^8−d^8 [Rh(I)−Rh(I)] complex with oxygen has been reported to result in a dinuclear [Rh(I)···Rh(III)(κ^2-O_2^{2-})] side-on peroxide complex.[25]

Reductive elimination and C−O bond formation from the side-on peroxo methyl complex (**E**) generates the final methylperoxo [M(II)OOCH$_3$] complex (**F**). The formation of C(sp^3)−O bonds via reductive elimination from high-valent platinum(IV) and palladium(IV) has been observed in several cases in recent years.[18,77−80] It is very likely that this final reductive elimination will only occur when the M−CH_3 bond is sufficiently weak, as is the case here for complexes [PtCH$_3$(**1**)](SbF$_6$), [PtCH$_3$(**2**)](SbF$_6$) and [PtCH$_3$(**4**)](SbF$_6$), where the steric hindrance created by the 6,6″-disubstituted terpyridine ligands forces the methyl group out of the coordination plane. We cannot exclude the possibility that, rather than the end-on peroxide complex **D**, the side-on peroxide complex [M(IV)(κ^2-O_2^{2-})] (**E**) undergoes reductive elimination and O═O bond formation, resulting in the generation of singlet oxygen.

■ CONCLUSIONS

The light-driven insertion of oxygen into a metal carbon bond has been investigated for a series of palladium(II) and platinum(II) methyl and phenyl complexes with substituted terpyridine and related tridentate bis(quinolyl)pyridine and bis(azaindole)pyridine ligands. The oxygen insertion reaction occurs readily for complexes which contain relatively bulky sp^2 hybridized (NH_2, NHMe) or sp^3 hybridized (CH_3) substituents in the 6,6″-positions of the terpyridine ligand, whereas smaller substituents such as H or CN result in inactive cases. Steric repulsion between these substituents and the metal methyl ligand results in a weakening of the metal carbon bond. Exposure of these complexes to oxygen and light results in the formation of methylperoxo platinum(II) and palladium(II) complexes. On the basis of crossover experiments using a labeled platinum complex and UV−vis spectroscopic studies, a mechanism is proposed whereby dinuclear triplet state complexes are generated upon irradiation, which react with triplet oxygen to generate superoxo and peroxo intermediates, eventually leading to the observed methylperoxo complexes in those complexes where the metal carbon bond is sufficiently weakened. DFT calculations and further spectroscopic studies are currently underway to support the proposed mechanism, and these will be discussed in our future reports.

dx.doi.org/10.1021/ja5055143 | J. Am. Chem. Soc. 2014, 136, 14089−14099

Table 1. Crystal Data, Data Collection, and Refinement Parameters for the Structures of $[Pt(CH_3)(2)](SbF_6)$, $[Pt(CH_3)(7)](SbF_6)$ and $[Pt(CH_3)(8)](SbF_6)$

data	$[Pt(CH_3)(2)]SbF_6$	$[Pt(CH_3)(7)]SbF_6$	$[Pt(CH_3)(8)]SbF_6$
formula	$[C_{18}H_{20}N_5Pt]SbF_6$	$[C_{24}H_{18}N_3Pt]SbF_6$	$[C_{20}H_{16}N_5Pt]SbF_6$
solvent	—	$0.9(C_3H_6O)$	—
formula weight	737.23	831.52	757.22
color, habit	orange needles	pale yellow blocks	pale yellow platy needles
crystal size/mm^3	0.46 × 0.07 × 0.03	0.35 × 0.25 × 0.11	0.23 × 0.11 × 0.03
temperature/K	173	173	173
crystal system	triclinic	triclinic	monoclinic
space group	$P\bar{1}$ (no. 2)	$P1$ (no. 1)	$P2_1/n$ (no. 14)
a/Å	7.86950(17)	8.92385(16)	11.82761(9)
b/Å	11.6934(3)	14.6411(3)	7.52718(6)
c/Å	12.1791(3)	21.3047(3)	24.4124(2)
α/deg	102.214(2)	91.8823(15)	—
β/deg	105.141(2)	100.5989(14)	93.9813(8)
γ/deg	99.416(2)	104.1322(17)	—
V/Å^3	1028.50(5)	2644.43(9)	2168.16(3)
Z	2	4[a]	4
D_c/g cm^{-3}	2.381	2.089	2.320
radiation used	Mo Kα	Mo Kα	Cu Kα
μ/mm^{-1}	8.176	6.374	22.427
2θ max/deg	66	65	145
no. of unique reflns			
measured (R_{int})	7067 (0.0295)	21515 (0.0180)	4255 (0.0317)
obs, $\|F_o\| > 4\sigma(\|F_o\|)$	6417	18042	3858
no. of variables	291	1533	369
R_1(obs), wR_2(all)[b]	0.0223, 0.0517	0.0338, 0.0871	0.0249, 0.0623

[a]There are four crystallographically independent complexes. [b]$R_1 = \Sigma||F_o| - |F_c||/\Sigma|F_o|$; $wR_2 = \{\Sigma[w(F_o^2 - F_c^2)^2]/\Sigma[w(F_o^2)^2]\}^{1/2}$; $w^{-1} = \sigma^2(F_o^2) + (aP)^2 + bP$.

EXPERIMENTAL SECTION

Details regarding the experimental techniques used, the synthesis of ligands and starting materials can be found in the Supporting Information.

Synthesis of Metal Complexes. *$[Pt(CH_3)(1)](BAr^F_4)$.* A Schlenk flask was loaded with $[PtCH_3(1)]Cl$ (0.152 g, 0.30 mmol) and $Na(BAr^F_4)$ (0.265 g, 0.30 mmol), in a glovebox, to which was added methanol (15 mL). The resulting suspension was stirred for 2 days, wrapped in aluminum foil. All volatile components were subsequently removed under a vacuum and dry acetone (15 mL) was added. The dark orange suspension was filtered via cannula and the remaining solid washed with dry acetone (15 mL). The acetone solution was reduced in volume leaving a sticky dark orange product. The product was triturated in hexane (2 × 15 mL) leaving behind a fine yellow powder, which was then dried under a vacuum. Yield: 0.326 g (82%). ^{1}H NMR (400 MHz, acetone-d_6) δ 8.43 (dd, J = 7.4, 8.7, 1H, H4′), 8.33 (d, J = 8.0, 2H, H3′, H5′), 7.90−7.82 (m, 2H, H4, H4″), 7.79 (s, 8H, BAr^F_4 o-H), 7.67 (s, 4H, BAr^F_4 p-H), 7.66 (m, 2H, H3, H3″), 7.13 (d, J = 8.8, 2H, H5, H5″), 6.90 (s, 4H, NH_2), 1.70 (s, $^2J_{PtH}$ = 73.6, 3H, $PtCH_3$). ^{13}C{^{1}H} NMR (100 MHz, acetone-d_6) δ 163.0, 162.6 (q, $^1J^{11}_{BC}$ = 49.9, BAr^F_4 i-C), 157.4, 154.2, 140.2, 140.1, 135.5 (s, BAr^F_4 o-C), 130.0 (q, $^2J_{CF}$ = 32.9, BAr^F_4 m-C), 125.3 (q, $^1J_{CF}$ = 271.8, BAr^F_4 CF_3), 123.6, 118.4, 116.4, 116.3, 114.5, −22.1 ($PtCH_3$). ^{19}F NMR (acetone-d_6) δ −63.3 (BAr^F_4, CF_3). MS (+LSIMS, m/z (%)): 473 (60) [(M-BAr^F_4)$^+$], 457 (60) [(M-CH_3−H-BAr^F_4)$^+$], 264 (40) [(6,6″-daterpy+H)$^+$]. MS (-LSIMS, m/z (%)): 863 (100) [$BAr^F_4{}^-$], 844 (5) [(BAr^F_4-F)$^-$]. Anal. Calcd For $C_{48}H_{28}N_5BF_{24}Pt$: C, 43.13; H, 2.11; N, 5.24. Found: C, 43.07; H, 2.07; N, 5.18.

$[Pt(CH_3)(2)](SbF_6)$. A Schlenk flask was charged with *trans*-$[PtCl(CH_3)(SMe_2)_2]$ (0.123 g, 0.33 mmol) and $AgSbF_6$ (0.114 g, 0.33 mmol). Dry acetone was (20 mL) added and the suspension was left to stir, covered in aluminum foil, for 30 min. The suspension was then filtered into another Schlenk flask, already containing a solution of 6,6″-di(methylamino)-2,2′:6′,2″-terpyridine (0.097 g, 0.33 mmol) in acetone (10 mL). The residue was washed with dry acetone (2 × 5 mL). The washings were combined with the initial acetone solution yielding an orange suspension. The suspension was left to stir overnight. The suspension was reduced to a minimum volume and the residue washed with DCM (5 mL) yielding an orange solid. Yield: 0.153 g (62%). Crystals suitable for X-ray analysis were grown from an acetone solution layered with pentane. ^{1}H NMR (500 MHz, CD_3CN) δ 8.13 (t, J = 8.1, 1H, H4′), 7.91 (d, J = 8.1, 2H, H3′, H5′), 7.76 (dd, J = 7.7, 8.4, 2H, H4, H4″), 7.27 (d, J = 7.2, 2H, H3, H3″), 6.78 (d, J = 8.9, 2H, H5, H5″), 6.16 (s, 2H, *H*NMe), 2.95 (d, J = 5.2, 6H, HN*Me*), 1.44 (s, $^2J_{PtH}$ = 72.6, 3H, $PtCH_3$). ^{13}C{^{1}H} NMR (125 MHz, CD_3CN) δ 161.3, 157.7, 154.2, 140.7, 139.9, 123.7, 113.8, 112.1, 30.1, −21.6 ($PtCH_3$). ^{19}F NMR (470 MHz, CD_3CN) δ −124.0 (superposition of a sextet due to $^{121}SbF_6^-$ and an octet due to $^{123}SbF_6^-$). MS (+LSIMS, m/z (%)): 501 (30) [(M-SbF_6)$^+$], 485 (15) [(M-CH_3−SbF_6)$^+$]. MS (-LSIMS, m/z (%)): 237 (70) [$^{123}SbF_6^-$], 235 (100) [$^{121}SbF_6^-$]. Anal. Calcd For $C_{18}H_{20}N_5F_6PtSb$: C, 29.33; H, 2.73; N, 9.50. Found: C, 29.41; H, 2.67; N, 9.53.

$[Pt(CH_3)(3)]Cl$. To a Schlenk flask containing *trans*-$[PtCl(CH_3)(SMe_2)_2]$ (0.049 g, 0.13 mmol) and 6-amino-2,2′:6′,2″-terpyridine (0.033 g, 0.13 mmol) DCM (20 mL) was added. The resultant yellow suspension was left to stir overnight. The suspension was then filtered, washed with diethyl ether (2 × 10 mL) and dried in vacuo yielding a bright yellow solid. Yield: 0.052 g (79%). ^{1}H NMR (400 MHz, CD_3OD) δ 8.58 (d, J = 5.5, $^3J_{PtH}$ = 48.5, 1H), 8.25 (td, J = 1.2, 7.7, 1H), 8.18 (d, J = 6.9, 1H), 8.14−8.06 (m, 2H), 7.97 (dd, J = 1.6, 7.1, 1H), 7.65 (ddd, J = 1.6, 5.8, 7.4, 1H), 7.60 (dd, J = 7.4, 8.4, 1H), 7.24 (dd, J = 0.8, 7.3, 1H), 6.77 (dd, J = 1.0, 8.6, 1H), 0.94 (s, $^2J_{PtH}$ = 67.6, 3H, $PtCH_3$). ^{13}C{^{1}H} NMR (100 MHz, CD_3OD) δ 164.1, 160.9, 157.2, 155.1, 152.5, 150.1, 141.8, 140.8, 140.3, 129.2, 126.1, 124.4, 123.7, 117.1, 115.2, −11.7 ($PtCH_3$). MS (+LSIMS, m/z (%)): 458 (100) [(M-Cl)$^+$], 442 (50) [(M-CH_3−Cl)$^+$]. Anal. Calcd For $C_{16}H_{15}N_4ClPt$: C, 38.91; H, 3.06; N, 11.34. Found: C, 38.79; H, 2.92; N, 11.21.

$[Pt(CH_3)(3)](SbF_6)$. A Schlenk flask was charged with $[PtCH_3(3)]Cl$ (0.040 g, 0.08 mmol) and $AgSbF_6$ (0.028 g, 0.08 mmol), to which dry methanol (10 mL) was added. The flask was wrapped in aluminum foil and the solution left to stir overnight. The resultant yellow suspension was reduced to a minimum volume. The residue was extracted with dry acetonitrile (10 mL) and filtered into a new Schlenk flask. The gray residue left behind was washed with acetonitrile (10 mL). The washings were combined with the initial acetonitrile extraction yielding a clear yellow solution. This solution was reduced to a minimum volume yielding a yellow solid. Yield: 0.034 g (61%). ^{1}H NMR (400 MHz, CD_3CN) δ 8.48 (d, J = 5.7, $^3J_{PtH}$ = 50.1, 1H), 8.16 (td, J = 1.3, 7.8, 1H), 8.04 (t, J = 8.1, 1H), 7.94 (d, J = 7.2, 1H), 7.86 (d, J = 8.0, 1H), 7.76 (d, J = 8.1, 1H), 7.56 (m, 2H), 7.09 (dd, J = 0.8, 7.3, 1H), 6.73 (dd, J = 1.0, 8.6, 1H), 5.87 (s, 2H, NH_2), 0.87 (s, $^2J_{PtH}$ = 68.4, 3H, $PtCH_3$). ^{13}C{^{1}H} NMR (125 MHz, CD_3CN) δ 163.4, 160.2, 156.7, 154.5, 152.0, 149.9, 141.6, 140.6, 140.3, 129.1, 125.8, 124.1, 123.4, 117.0, 115.3, −11.7 ($PtCH_3$). ^{19}F NMR (376 MHz, CD_3CN) δ −122.5 (superposition of a sextet due to $^{121}SbF_6^-$ and an octet due to $^{123}SbF_6^-$). MS (+ESI, m/z (%)): 458 (100) [(M-SbF_6)$^+$]. MS (-ESI, m/z (%)): 237 (70) [$^{123}SbF_6^-$], 235 (100) [$^{121}SbF_6^-$].

$[Pt(CH_3)(4)](SbF_6)$. A Schlenk flask was charged with *trans*-$[PtCl(CH_3)(SMe_2)_2]$ (0.111 g, 0.30 mmol) and $AgSbF_6$ (0.103 g, 0.30 mmol). Next dry acetone (10 mL) was added and the suspension was left to stir, covered in aluminum foil, for 30 min. The suspension was filtered into another Schlenk flask containing 6,6″-dimethyl-2,2′:6′,2″-terpyridine **4** (0.078 g, 0.30 mmol). The residue was washed with dry acetone (5 mL). The washings were combined with the initial acetone solution yielding an orange suspension. The suspension was

dx.doi.org/10.1021/ja5055143 | J. Am. Chem. Soc. 2014, 136, 14089−14099

left to stir overnight and subsequently reduced to a minimum volume. The product was washed with dry DCM (2 × 5 mL) and dried under a vacuum yielding a yellow solid. Yield: 0.129 g (61%). ^{1}H NMR (400 MHz, acetone-d_6) δ 8.58 (m, 3H, H3′, H4′, H5′), 8.44 (d, J = 6.6, 2H, H3, H3″), 8.33 (t, J = 7.8, 2H, H4, H4″), 7.90 (dd, J = 7.9, 1.4, 2H, H5, H5″), 2.99 (s, 6H, Me), 1.76 (s, $^2J_{PtH}$ = 77.2, 3H, $PtCH_3$). $^{13}C\{^1H\}$ NMR (100 MHz, acetone-d_6) δ 167.5, 161.0, 153.9, 141.1, 140.6, 130.9, 124.9, 123.3, 27.7, −12.6 ($PtCH_3$). ^{19}F NMR (376 MHz, acetone-d_6) δ −122.4 (superposition of a sextet due to $^{121}SbF_6^-$ and an octet due to $^{123}SbF_6^-$). MS (+ESI, m/z (%)): 472 (87) [(M-SbF_6)$^+$], 471 (100) [(M-SbF_6)$^+$], 470 (84) [(M-SbF_6)$^+$]. Anal. Calcd For $C_{18}H_{18}N_3F_6PtSb$: C, 30.57; H, 2.57; N, 5.94. Found: C, 30.69; H, 2.49; N, 5.87.

*[Pt(CH$_3$)(**5**)](SbF$_6$).* A Schlenk flask was charged with 6,6″-dicyano-2,2′:6′,2″-terpyridine (0.038 g, 0.14 mmol), *trans*-[PtCl(CH_3)-(SMe_2)$_2$] (0.050 g, 0.14 mmol) and $AgSbF_6$ (0.047 g, 0.14 mmol) to which dry acetone (5 mL) was added. The flask was wrapped in aluminum foil and the suspension left to stir overnight. The resultant orange suspension was filtered into a new Schlenk flask. The residue left behind was washed with dry acetone (2 × 5 mL). The washings were combined with the initial acetone solution yielding a clear orange solution, which was reduced to a minimum volume yielding an orange residue. The product was washed with dry DCM (2 × 5 mL) and dried under a vacuum yielding a pale orange solid. Yield: 0.009 g (9%). ^{1}H NMR (400 MHz, acetone-d_6) δ 8.97 (dd, J = 8.1, 1.4, 2H, H3, H3″), 8.87 (d, J = 7.8, 2H, H3′, H5′), 8.83 (t, J = 8.0, 2H, H4, H4″), 8.76 (dd, J = 8.8, 7.3, 1H, H4′), 8.53 (dd, J = 7.8, 1.4, 2H, H5, H5″), 2.09 (s, $^2J_{PtH}$ = 76.1, 3H, $PtCH_3$). $^{13}C\{^1H\}$ NMR (100 MHz, acetone-d_6) δ 163.9, 152.3, 143.3, 142.0, 137.8, 137.6, 129.6, 126.7, 115.4, −3.1 ($^1J_{PtC}$ = 711.5, $PtCH_3$). ^{19}F NMR (376 MHz, acetone-d_6) δ −123.7 (superposition of a sextet due to $^{121}SbF_6^-$ and an octet due to $^{123}SbF_6^-$). MS (+LSIMS, m/z (%)): 493 (15) [(M-SbF_6)$^+$], 477 (15) [(M-CH_3−SbF_6)$^+$]. MS (-LSIMS, m/z (%)): 237 (75) [$^{123}SbF_6^-$], 235 (100) [$^{121}SbF_6^-$].

*[Pd(CH$_3$)(**7**)](SbF$_6$).* A Schlenk flask was charged with 2,6-di(8′-quinolinyl)pyridine (**7**) (0.063 g, 0.19 mmol), [$PdCl(CH_3)$(1,5-COD)] (0.050 g, 0.19 mmol) and $AgSbF_6$ (0.065 g, 0.19 mmol) to which dry acetone (10 mL) was added. The Schlenk flask was wrapped in aluminum foil and the suspension left to stir overnight. The resultant black suspension was filtered into a new Schlenk flask. The residue left behind was washed with dry acetone (2 × 10 mL). The washings were combined with the initial acetone solution and reduced to a minimum yielding a pale yellow solid. The product was triturated in pentane, leaving behind a beige solid which was dried in vacuo. Yield: 0.077 g (59%). ^{1}H NMR (400 MHz, acetone-d_6) δ 9.12 (dd, J = 5.1, 1.5, 2H, H2), 8.94 (dd, J = 8.3, 1.5, 2H, H4), 8.82 (dd, J = 7.4, 1.3, 2H, H7), 8.48 (dd, J = 8.2, 1.3, 2H, H5), 8.40 (dd, J = 8.5, 7.6, 1H, H4′), 8.25 (d, J = 8.1, 2H, H3′), 8.12−8.05 (m, 2H, H6), 7.86 (dd, J = 8.2, 5.1, 2H, H3), 0.15 (s, 3H, $PdCH_3$). $^{13}C\{^1H\}$ NMR (100 MHz, acetone-d_6) δ 158.1, 152.4, 144.4, 142.0, 141.4, 135.2, 133.8, 133.2, 130.3, 129.2, 127.6, 123.5, 5.7 ($PdCH_3$). ^{19}F NMR (376 MHz, acetone-d_6) δ −122.4 (superposition of a sextet due to $^{121}SbF_6^-$ and an octet due to $^{123}SbF_6^-$). MS (+LSIMS, m/z (%)): 454 (50) [(M-SbF_6)$^+$], 438 (40) [(M-CH_3−SbF_6)$^+$]. MS (-LSIMS, m/z (%)): 237 (75) [$^{123}SbF_6^-$], 235 (100) [$^{121}SbF_6^-$]. Anal. Calcd For $C_{24}H_{18}N_3F_6PdSb$: C, 41.74; H, 2.63; N, 6.08. Found: C, 41.84; H, 2.56; N, 5.97.

*[Pt(CH$_3$)(**7**)](SbF$_6$).* A Schlenk flask was charged with 2,6-di(8′-quinolinyl)pyridine (**7**) (0.045 g, 0.14 mmol), *trans*-[PtCl(CH_3)-(SMe_2)$_2$] (0.050 g, 0.14 mmol) and $AgSbF_6$ (0.047 g, 0.14 mmol) to which dry acetone (15 mL) was added. The Schlenk flask was wrapped in aluminum foil and the suspension left to stir overnight. The resultant yellow suspension was filtered into a new Schlenk flask. The residue left behind was washed with dry acetone (2 × 10 mL). The washings were combined with the initial acetone solution yielding a clear yellow solution which was reduced to a minimum volume yielding a yellow solid. The product was dissolved in a minimum amount of dry acetone and precipitated with dry diethyl ether. The suspension was filtered, washed with dry diethyl ether (2 × 5 mL) and dried under a vacuum yielding a yellow solid. Yield: 0.071 g (67%). Crystals suitable for X-ray analysis were grown from an acetone solution layered with hexane. ^{1}H NMR (500 MHz, acetone-d_6) δ 9.22 (dd, J = 1.5, 5.3, $^3J_{PtH}$ = 63.3, 2H, H2), 8.96 (dd, J = 1.4, 8.2, 2H, H4), 8.87 (dd, J = 1.3, 7.4, 2H, H7), 8.49 (dd, J = 1.3, 8.2, 2H, H5), 8.44 (dd, J = 7.7, 8.5, 1H, H4′), 8.31 (d, J = 8.1, 2H, H3′), 8.06 (dd, J = 7.6, 8.0, 2H, H6), 7.77 (dd, J = 5.3, 8.2, 2H, H3), 0.55 (s, $^2J_{PtH}$ = 71.2, 3H, $PtCH_3$). $^{13}C\{^1H\}$ NMR (125 MHz, acetone-d_6) δ 157.4, 151.5, 144.8, 141.2, 141.1, 134.4, 134.0, 132.7, 130.4, 129.7, 127.8, 124.3 (J_{PtC} = 58.1), −4.1 ($PtCH_3$). ^{19}F NMR (470 MHz, acetone-d_6) δ −123.4 (superposition of a sextet due to $^{121}SbF_6^-$ and an octet due to $^{123}SbF_6^-$). MS (+LSIMS, m/z (%)): 543 (10) [(M-SbF_6)$^+$], 527 (20) [(M-CH_3−SbF_6)$^+$]. MS (-LSIMS, m/z (%)): 237 (70) [$^{123}SbF_6^-$], 235 (100) [$^{121}SbF_6^-$]. Anal. Calcd For $C_{24}H_{18}N_3F_6PtSb$: C, 36.99; H, 2.33; N, 5.39. Found: C, 37.06; H, 2.22; N, 5.30.

*[Pt(CH$_3$)(**8**)](SbF$_6$).* A Schlenk flask was charged with 2,6-di(N-7-azaindolyl)pyridine (**8**) (0.042 g, 0.14 mmol), *trans*-[PtCl(CH_3)-(SMe_2)$_2$] (0.050 g, 0.14 mmol) and $AgSbF_6$ (0.047 g, 0.14 mmol) to which dry acetone (15 mL) was added. The flask was wrapped in aluminum foil and the suspension left to stir overnight. The resultant pale yellow suspension was filtered into a new Schlenk flask. The residue left behind was washed with dry acetone (2 × 5 mL). The washings were combined with the initial acetone solution yielding a clear pale yellow solution which was reduced to a minimum volume yielding a pale yellow solid. The product was dissolved in a minimum amount of dry acetone and precipitated with dry diethyl ether. The suspension was filtered, washed with dry diethyl ether (2 × 5 mL) and dried under a vacuum yielding an off-white solid. Yield: 0.052 g (51%). Crystals suitable for X-ray analysis were grown from an acetone solution layered with hexane. ^{1}H NMR (400 MHz, acetone-d_6) δ 8.66 (d, J = 5.9, $^3J_{PtH}$ = 53.4, 2H, H2), 8.55 (dd, J = 1.1, 7.8, 2H, H4), 8.47 (d, J = 4.0, 2H, H6), 8.45 (t, J = 8.3, 1H, H4′). 7.93 (d, J = 8.3, 2H, H3′), 7.58 (dd, J = 5.9, 7.7, 2H, H3), 7.31 (d, J = 4.0, 2H, H5), 1.12 (s, $^2J_{PtH}$ = 78.0, 3H, $PtCH_3$). $^{13}C\{^1H\}$ NMR (100 MHz, acetone-d_6) δ 147.4, 146.5, 146.3, 143.8, 134.3, 130.2, 126.7, 121.6, 115.4, 109.9, −6.7 ($PtCH_3$). ^{19}F NMR (376 MHz, acetone-d_6) δ −122.4 (superposition of a sextet due to $^{121}SbF_6^-$ and an octet due to $^{123}SbF_6^-$). MS (+LSIMS, m/z (%)): 521 (30) [(M-SbF_6)$^+$], 505 (20) [(M-CH_3−SbF_6)$^+$]. MS (-LSIMS, m/z (%)): 237 (75) [$^{123}SbF_6^-$], 235 (100) [$^{121}SbF_6^-$]. Anal. Calcd For $C_{20}H_{16}N_5F_6PtSb$: C, 31.72; H, 2.13; N, 9.25. Found: C, 31.75; H, 2.10; N, 9.18.

General Procedure for the Formation of Methylperoxo Complexes. In a normal NMR tube, the complex (∼2 mg) is dissolved in CD_3CN or CD_3COCD_3 (0.5 mL) to give a clear solution. After bubbling O_2 through the solution for approximately 1 min at room temperature, the NMR tube is exposed to sunlight for 1 min or UV light (365 nm, 100W) until the starting methyl complex is completely converted to the methylperoxo complex. The methyl peroxo complexes are generally unstable, in particular those with bulkier substituents in the 6,6″-positions of the ligand such as **2** and **4**, and further exposure to light leads to decomposition. The NMR data for complex [Pt($OOCH_3$)(**1**)](SbF_6) have been reported previously.[34]

[Pt($OOCH_3$)(**2**)](SbF_6) (see Figure S9 (SI)): ^{1}H NMR (400 MHz, CD_3CN) δ 9.7 (br s, 2H, *H*NMe), 8.10 (t, J = 8, 1H, H4′), 7.75 (d, J = 8, 2H, H3′, H5′), 7.63 (dd, J = 8, 9, 2H, H4, H4″), 7.10 (d, J = 7, 2H, H3, H3″), 6.60 (d, J = 9, 2H, H5, H5″), 3.60 (s, 3H, PtOOC*H*$_3$), 2.76 (d, J = 5, 6H, HN*Me*).

[Pt($OOCH_3$)(**4**)](SbF_6) (see Figure S10 (SI)): ^{1}H NMR (400 MHz, CD_3COCD_3) δ 8.56 (m, H3′, H4′, H5′), 8.47 (dd, J = 7, 7, 2H, H4, H4″), 7.10 (d, J = 7, 2H, H3, H3″), 7.88 (d, J = 7, 2H, H5, H5″), 3.82 (s, 3H, PtOOC*H*$_3$), 3.21 (s, 6H, C*H*$_3$).

[Pd($OOCH_3$)(**1**)](SbF_6) (see Figure S11 (SI)): ^{1}H NMR (400 MHz, CD_3CN) δ 8.12 (t, J = 8, 1H, H4′), 7.83 (d, J = 8, 2H, H3′, H5′), 7.60 (dd, J = 8, 9, 2H, H4, H4″), 7.18 (d, J = 7, 2H, H3, H3″), 6.70 (d, J = 9, 2H, H5, H5″), 3.72 (s, 3H, OOC*H*$_3$). ^{13}C NMR (HMQC, CD_3CN): 139.5 (*C*H4,H4″), 122.0 (*C*H3′,H5′), 117.1 (*C*H5,H5″), 112.1 (*C*H3,H3″), 63.6 (OO*C*H$_3$).

Crystallography. Table 1 provides a summary of the crystallographic data for the structures of [Pt(CH_3)(**2**)](SbF_6), [Pt(CH_3)-(**7**)](SbF_6) and [Pt(CH_3)(**8**)](SbF_6). Data were collected using Oxford Diffraction Xcalibur 3S ([Pt(CH_3)(**2**)](SbF_6), [Pt(CH_3)(**7**)]-

dx.doi.org/10.1021/ja5055143 | J. Am. Chem. Soc. 2014, 136, 14089−14099

(SbF_6)) and Xcalibur PX Ultra ([$Pt(CH_3)$(**8**)](SbF_6)) diffractometers, and the structures were refined based on F^2 using the SHELXTL, SHELX-97, and SHELX-2013 program systems.[81] The absolute structure of [$Pt(CH_3)$(**7**)](SbF_6) was determined by a combination of *R*-factor tests [$R_1^+ = 0.0338$, $R_1^- = 0.0353$] and by use of the Flack parameter [$x^+ = 0.309(5)$] (see the Supporting Information for more details). CCDC 987854 to 987856.

■ ASSOCIATED CONTENT

Supporting Information

X-ray crystallographic files in CIF format and experimental details regarding the synthesis and characterization of the ligands and metal complexes, including spectroscopic details. This material is available free of charge via the Internet at http://pubs.acs.org.

■ AUTHOR INFORMATION

Corresponding Author

g.britovsek@imperial.ac.uk

Notes

The authors declare no competing financial interest.

■ ACKNOWLEDGMENTS

We are grateful to EPSRC and BP for funding. We thank Johnson Matthey for a generous loan of palladium and platinum salts. Prof. Allan Canty is thanked for very helpful discussions.

■ REFERENCES

(1) Crabtree, R. H. *J. Chem. Soc., Dalton Trans.* **2001**, 2437.
(2) Stahl, S. S.; Labinger, J. A.; Bercaw, J. E. *Angew. Chem., Int. Ed.* **1998**, *37*, 2180.
(3) Fekl, U.; Goldberg, K. I. *Adv. Inorg. Chem.* **2003**, *54*, 259.
(4) Lersch, M.; Tilset, M. *Chem. Rev.* **2005**, *105*, 2471.
(5) Vedernikov, A. N. *Acc. Chem. Res.* **2012**, *45*, 803.
(6) Boisvert, L.; Goldberg, K. I. *Acc. Chem. Res.* **2012**, *45*, 899.
(7) Pellarin, K. R.; McCready, M. S.; Puddephatt, R. J. *Organometallics* **2012**, *31*, 6388.
(8) Rostovtsev, V. V.; Henling, L. M.; Labinger, J. A.; Bercaw, J. E. *Inorg. Chem.* **2002**, *41*, 3608.
(9) Lyons, T. W.; Sanford, M. S. *Chem. Rev.* **2010**, *110*, 1147.
(10) Canty, A. J. *Dalton Trans.* **2009**, 10409.
(11) Bandoli, G.; Caputo, P. A.; Intini, F. P.; Sivo, M.; Natile, G. *J. Am. Chem. Soc.* **1997**, *119*, 10370.
(12) Powers, D. C.; Ritter, T. *Nat. Chem.* **2009**, *1*, 302.
(13) Deprez, N. R.; Sanford, M. S. *J. Am. Chem. Soc.* **2009**, *131*, 11234.
(14) Canty, A. J.; Gardiner, M. G.; Jones, R. C.; Rodemann, T.; Sharma, M. *J. Am. Chem. Soc.* **2009**, *131*, 7236.
(15) Bonnington, K. J.; Jennings, M. C.; Puddephatt, R. J. *Organometallics* **2008**, *27*, 6521.
(16) Ye, Y.; Ball, N. D.; Kampf, J. W.; Sanford, M. S. *J. Am. Chem. Soc.* **2010**, *132*, 14682.
(17) Mirica, L. M.; Khusnutdinova, J. R. *Coord. Chem. Rev.* **2013**, *257*, 299.
(18) Powers, D. C.; Lee, E.; Ariafard, A.; Sanford, M. S.; Yates, B. F.; Canty, A. J.; Ritter, T. *J. Am. Chem. Soc.* **2012**, *134*, 12002.
(19) Powers, D. C.; Ritter, T. *Acc. Chem. Res.* **2012**, *45*, 840.
(20) Landis, C. R.; Morales, C. M.; Stahl, S. S. *J. Am. Chem. Soc.* **2004**, *126*, 16302.
(21) Valentine, J. S. *Chem. Rev.* **1973**, *73*, 235.
(22) Djurovich, P. I.; Murphy, D.; Thompson, M. E.; Hernandez, B.; Gao, R.; Hunt, P. L.; Selke, M. *Dalton Trans.* **2007**, 3763.
(23) Zhang, D.; Wu, L.-Z.; Yang, Q.-Z.; Li, X.-H.; Zhang, L.-P.; Tung, C.-H. *Org. Lett.* **2003**, *5*, 3221.
(24) Li, X.-H.; Wu, L.-Z.; Zhang, L.-P.; Tung, C.-H.; Che, C.-M. *Chem. Commun.* **2001**, 2280.
(25) Ho, D. G.; Ismail, R.; Franco, N.; Gao, R.; Leverich, E. P.; Tsyba, I.; Ho, N. N.; Bau, R.; Selke, M. *Chem. Commun.* **2002**, 570.
(26) Selke, M.; Foote, C. S. *J. Am. Chem. Soc.* **1993**, *115*, 1166.
(27) Frech, C. M.; Shimon, L. J. W.; Milstein, D. *Helv. Chim. Acta* **2006**, *89*, 1730.
(28) Praetorius, J. M.; Allen, D. P.; Wang, R.; Webb, J. D.; Grein, F.; Kennepohl, P.; Crudden, C. M. *J. Am. Chem. Soc.* **2008**, *130*, 3724.
(29) Cipot-Wechsler, J.; Covelli, D.; Praetorius, J. M.; Hearns, N.; Zenkina, O. V.; Keske, E. C.; Wang, R.; Kennepohl, P.; Crudden, C. M. *Organometallics* **2012**, *31*, 7306.
(30) Wouters, J. M. A.; Vrieze, K.; Elsevier, C. J.; Zoutberg, M. C.; Goubitz, K. *Organometallics* **1994**, *13*, 1510.
(31) Connick, W. B.; Gray, H. B. *J. Am. Chem. Soc.* **1997**, *119*, 11620.
(32) Zhang, Y.; Ley, K. D.; Schanze, K. S. *Inorg. Chem.* **1996**, *35*, 7102.
(33) Hu, J.; Xu, H.; Nguyen, M.-H.; Yip, J. H. K. *Inorg. Chem.* **2009**, *48*, 9684.
(34) Taylor, R. A.; Law, D. J.; Sunley, G. J.; White, A. J. P.; Britovsek, G. J. P. *Angew. Chem., Int. Ed.* **2009**, *48*, 5900.
(35) Grice, K. A.; Goldberg, K. I. *Organometallics* **2009**, *28*, 953.
(36) Boisvert, L.; Denney, M. C.; Hanson, S. K.; Goldberg, K. I. *J. Am. Chem. Soc.* **2009**, *131*, 15802.
(37) Petersen, A. R.; Taylor, R. A.; Vicente-Hernández, I.; Heinzer, J.; White, A. J. P.; Britovsek, G. J. P. *Organometallics* **2014**, *33*, 1453.
(38) Romeo, R.; Scolaro, L. M.; Plutino, M. R.; Albinati, A. *J. Organomet. Chem.* **2000**, *593*−*594*, 403.
(39) Garner, K. L.; Parkes, L. F.; Piper, J. D.; Williams, J. A. G. *Inorg. Chem.* **2010**, *49*, 476.
(40) Abrahamsson, M.; Jäger, M.; Österman, T.; Eriksson, L.; Persson, P.; Becker, H. C.; Johansson, O.; Hammarström, L. *J. Am. Chem. Soc.* **2006**, *128*, 12616.
(41) Jäger, M.; Eriksson, L.; Bergquist, J.; Johansson, O. *J. Org. Chem.* **2007**, *72*, 10227.
(42) Collins, S. N.; Taylor, S.; Krause, J. A.; Connick, W. B. *Acta Crystallogr., Sect. C: Cryst. Struct. Commun.* **2007**, *63*, m436.
(43) Hoang, T. N. Y.; Lathion, T.; Guénée, L.; Terazzi, E.; Piguet, C. *Inorg. Chem.* **2012**, *51*, 8567.
(44) Houlding, V. H.; Miskowski, V. M. *Coord. Chem. Rev.* **1991**, *111*, 145.
(45) Bailey, J. A.; Hill, M. G.; Marsh, R. E.; Miskowski, V. M.; Schaefer, W. P.; Gray, H. B. *Inorg. Chem.* **1995**, *34*, 4591.
(46) Bercaw, J. E.; Durrell, A. C.; Gray, H. B.; Green, J. C.; Hazari, N.; Labinger, J. A.; Winkler, J. R. *Inorg. Chem.* **2010**, *49*, 1801.
(47) Smith, D. C.; Gray, H. B. *Chem. Soc. Rev.* **1990**, *100*, 169.
(48) Marino, N.; Fazen, C. H.; Blakemore, J. D.; Incarvito, C. D.; Hazari, N.; Doyle, R. P. *Inorg. Chem.* **2011**, *50*, 2507.
(49) Luo, J.; Khusnutdinova, J. R.; Rath, N. P.; Mirica, L. M. *Chem. Commun.* **2012**, *48*, 1532.
(50) Arena, G.; Monsú Scolaro, L.; Pasternack, R. F.; Romeo, R. *Inorg. Chem.* **1995**, *34*, 2994.
(51) Arena, G.; Calogero, G.; Campagna, S.; Monsú Scolaro, L.; Ricevuto, V.; Romeo, R. *Inorg. Chem.* **1998**, *37*, 2763.
(52) Lai, S.-W.; Chan, M. C. W.; Cheung, K.-K.; Che, C.-M. *Inorg. Chem.* **1999**, *38*, 4262.
(53) Zhang, H.-X.; Kato, M.; Sasaki, Y.; Ohba, T.; Ito, H.; Kobayashi, A.; Chang, H.-C.; Uosaki, K. *Dalton Trans.* **2012**, *41*, 11497.
(54) Cummings, S. D. *Coord. Chem. Rev.* **2009**, *253*, 449.
(55) McGuire, R., Jr; McGuire, M. C.; McMillin, D. R. *Coord. Chem. Rev.* **2010**, *254*, 2574.
(56) Klein, A.; van Slageren, J.; Zalis, S. *Inorg. Chem.* **2002**, *41*, 5216.
(57) van Slageren, J.; Klein, A.; Zalis, S. *Coord. Chem. Rev.* **2002**, *230*, 193.
(58) Hackett, M.; Whitesides, G. M. *J. Am. Chem. Soc.* **1988**, *110*, 1449.
(59) Hill, G. S.; Puddephatt, R. J. *Organometallics* **1998**, *17*, 1478.
(60) Ananikov, V. P.; Musaev, D. G.; Morokuma, K. *Organometallics* **2005**, *24*, 715.

(61) Aye, K.-T.; Canty, A. J.; Crespo, M.; Puddephatt, R. J.; Scott, J. D.; Watson, A. A. *Organometallics* **1989**, *8*, 1518.
(62) Hess, A.; Horz, M. A.; Liable-Sands, L. M.; Lindner, D. C.; Rheingold, A. L.; Theopold, K. H. *Angew. Chem., Int. Ed.* **1999**, *38*, 166.
(63) Crites, D. K.; Cunningham, C. T.; McMillin, D. R. *Inorg. Chim. Acta* **1998**, *273*, 346.
(64) Rinalducci, S.; Pedersen, J. Z.; Zolla, L. *Biochim. Biophys. Acta* **2004**, *1608*, 63.
(65) Ogilby, P. R.; Foote, C. S. *J. Am. Chem. Soc.* **1983**, *105*, 3423.
(66) Aldridge, T. K.; Stacy, E. M.; McMillin, D. R. *Inorg. Chem.* **1994**, *33*, 722.
(67) McMillin, D. R.; Moore, J. J. *Coord. Chem. Rev.* **2002**, *229*, 113.
(68) Yam, V. W.-W.; Wong, K. M.-C.; Zhu, N. *J. Am. Chem. Soc.* **2002**, *124*, 6506.
(69) Miskowski, V. M.; Rice, S. F.; Gray, H. B.; Dallinger, R. F.; Milder, S. J.; Hill, M. G.; Exstrom, C. L.; Mann, K. R. *Inorg. Chem.* **1994**, *33*, 2799.
(70) Bercaw, J. E.; Durrell, A. C.; Gray, H. B.; Green, J. C.; Hazari, N.; Labinger, J. A.; Winkler, J. R. *Inorg. Chem.* **2010**, *49*, 1801.
(71) Hill, M. G.; Mann, K. R. *Catal. Lett.* **1991**, *11*, 341.
(72) Powers, D. C.; Geibel, M. A. L.; Klein, J. E. M. N.; Ritter, T. *J. Am. Chem. Soc.* **2009**, *131*, 17050.
(73) Ariafard, A.; Hyland, C. J. T.; Canty, A. J.; Sharma, M.; Yates, B. F. *Inorg. Chem.* **2011**, *50*, 6449.
(74) Khusnutdinova, J. R.; Rath, N. P.; Mirica, L. M. *J. Am. Chem. Soc.* **2012**, *134*, 2414.
(75) Ariafard, A.; Hyland, C. J. T.; Canty, A. J.; Sharma, M.; Brookes, N. J.; Yates, B. F. *Inorg. Chem.* **2010**, *49*, 11249.
(76) DeRosa, M. C.; Crutchley, R. J. *Coord. Chem. Rev.* **2002**, *233*−*234*, 351.
(77) Vedernikov, A. N. *Top. Organomet. Chem.* **2010**, *31*, 101.
(78) Dick, A. R.; Kampf, J. W.; Sanford, M. S. *J. Am. Chem. Soc.* **2005**, *127*, 12790.
(79) Racowski, J. M.; Dick, A. R.; Sanford, M. S. *J. Am. Chem. Soc.* **2009**, *131*, 10974.
(80) Williams, B. S.; Goldberg, K. I. *J. Am. Chem. Soc.* **2001**, *123*, 2576.
(81) SHELXTL, Bruker AXS, Madison, WI; SHELX-97, Sheldrick, G. M. *Acta Cryst.* **2008**, *A64*, 112; SHELX-2013, http://shelx.uni-ac.gwdg.de/SHELX/index.php.